

**Griffith, Muir, Suchanek et al. Supplementary information**

**Figure S1– Clinical characteristics of bnAb donor T125 and and epitope specificity of ELC07**

**Figure S2 – Figure S2. Cryo-EM structure of HIV-1 Env in complex with ELC07 Fab**

**Figure S3– B cell subset distributions in the ELC07 bnAb donor**

**Figure S4 – Comparison of HIV-1 Env reactive IgG+ B cells from BnAb donor and total memory B cells from the reference donor**

**Figure S5 – Integration of publicly available data from HIV-negative controls and individuals living with HIV-1 viremia**

**Table S1 – Cryo-EM data collection, image processing and model refinement.**

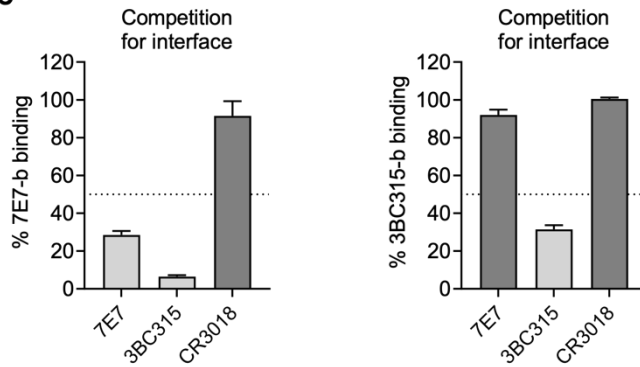
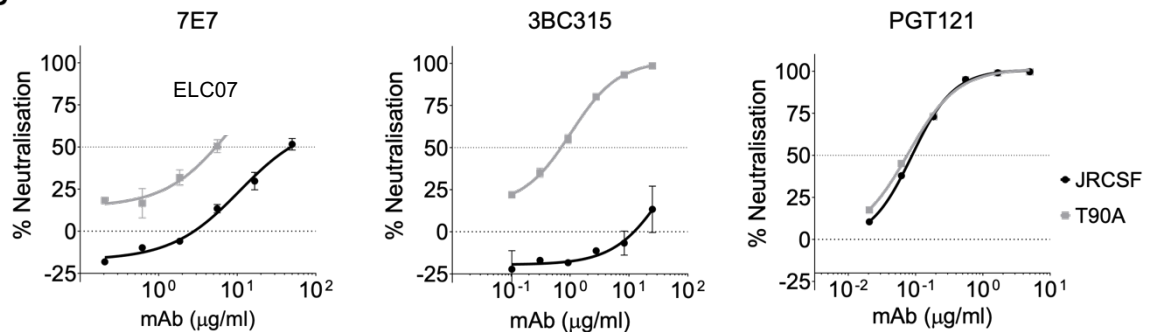
**References**

**A**

Patient ID	T125
Gender	Male
Country of birth	Sri Lanka
HIV clade	C
EC / LTNP	No
Year of sampling	2009
Age at sampling	37
Viral load	73700
CD4 count	Unknown
Neutralisation score	3.19

**B**

Epitope	PV mutation or protein absorption	Fold change in ID <sub>50</sub> titre
gp120	BG505 gp120 absorption	2.5
High mannose patch	JRCSF N332A/N295A	1.0
Trimer apex	CRF250-4 N160A/K169T	8.0
CD4bs	JRCSF D279A	1.0
	BG505 N276D/N462D	4.2
Fusion peptide	JRCSF T90A	1.1
MPER	JRCSF MPER absorption	0.9

**C****D**

**Figure S1– Clinical characteristics and epitope specificity of bnAb donor T125 and ELC07 – related to Figure 1**

**(A)** Demographic characteristics and clinical features for elite neutraliser T125. **(B)** Effect of protein absorption or PV mutation on plasma neutralisation by elite neutraliser T125, with a 3 fold-change in ID<sub>50</sub> titer compared to the wild-type (WT) PV or condition highlighted.

**(C)** Percentage binding of biotinylated ELC07 and 3BC315 to the gp120-gp41 interface of BG505 SOSIP in reciprocal competition ELISAs, mAbs were tested in duplicate with the mean and error bars shown. The non- mAb CR3018 was included as a negative control and a dotted line at 50% indicates the threshold for competitive binding. **(D)** Neutralisation curves of bnAbs ELC07, 3BC315 and PGT121 titrated in duplicate against JRCSF PV (black) and a T90A mutated version (grey) to remove the glycan site at position 88, with the mean and error bars shown. Dotted lines to indicate 0% and 50% neutralisation.

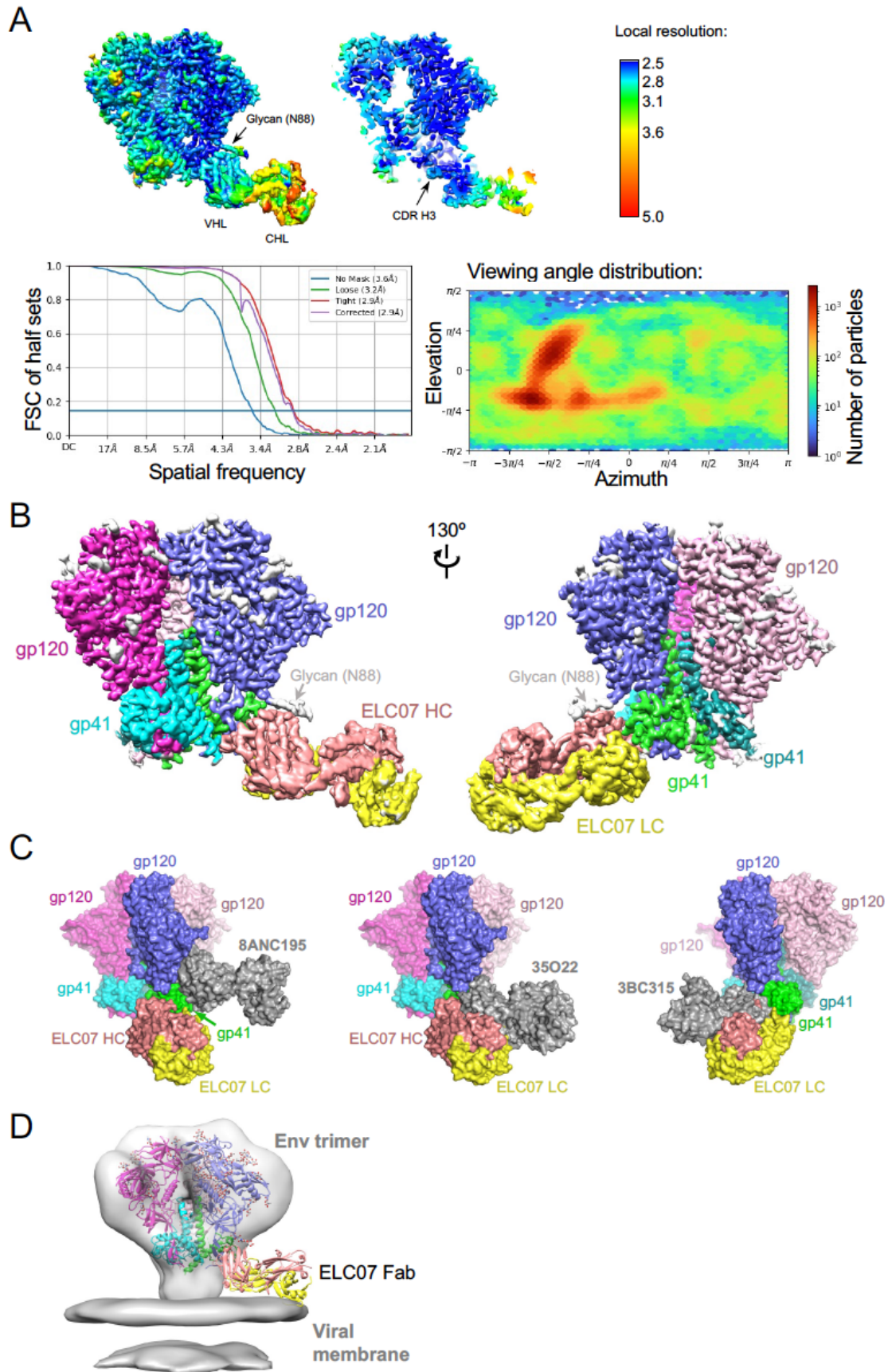


**Figure S2. Cryo-EM structure of HIV-1 Env in complex with ELC07 Fab.**

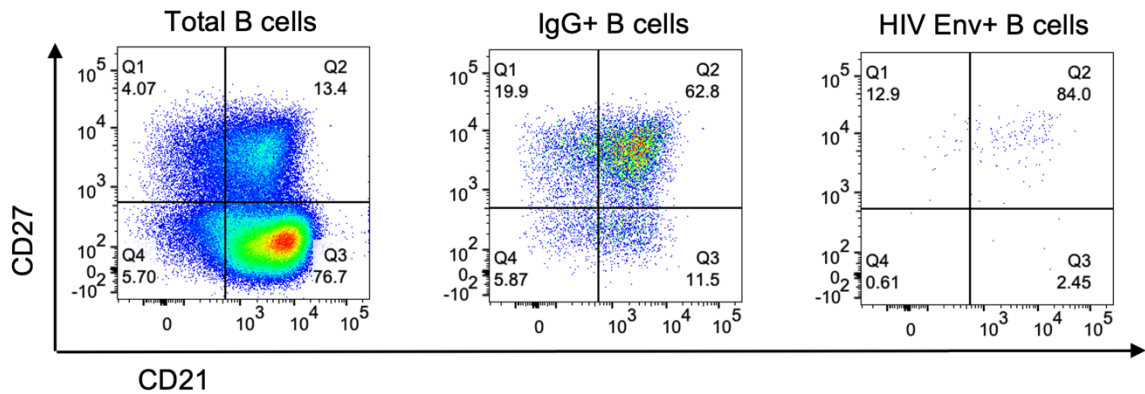
(A) Top panels show the cryo-EM map locally filtered using DeepEMhancer<sup>1</sup> and coloured by local resolution (as indicated on the inset on the right). The middle panel shows a slice through the map with features representing variable (VHL) and constant (CHL), and the CDR H3 loop indicated. Bottom left panel shows half-map Fourier shell correlation (FSC) without mask (blue line), with loose mask (green line), with tight mask (red line), and optimised mask (purple line). The FSC threshold of 0.143 (horizontal blue line) corresponds to 2.9 Å global resolution of 2.9 Å. Bottom right panel shows the viewing angle distribution of assigned to individual particle images that contributed to the final 3D reconstruction.

(B) Cryo-EM map coloured by protein chain as in Fig1, viewed in two orientations related by 130-Å rotation, as indicated.

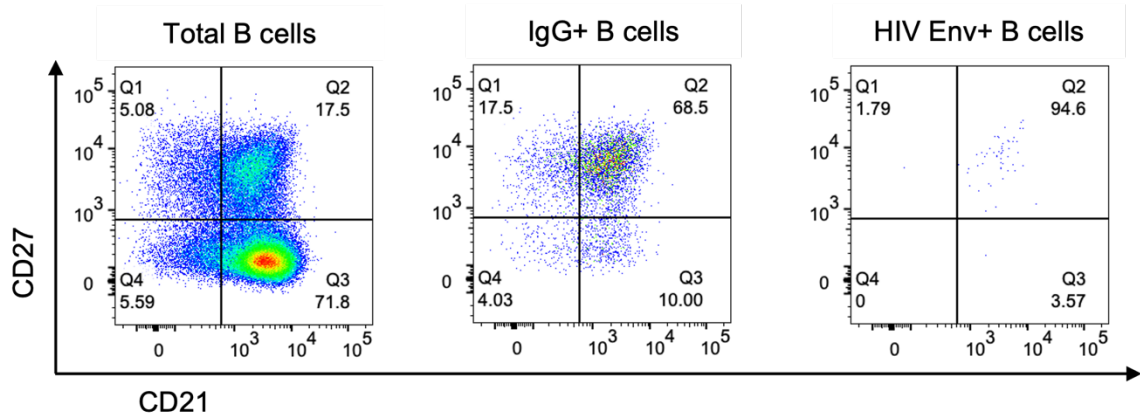
(C) Comparison of ELC07 to other characterised bnAbs that target the gp120-gp41 interface. The reconstruction of the Env in complex with ELC07 (coloured as in Fig1) is shown superposed on Env in complex with 8ANC195 (PDB ID 5CJX<sup>2</sup>, left), 35O22 (PDB ID 4TVP<sup>3</sup>, middle), or 3BC315 (EMBD ID 3067, PDB ID 5CCK (26404402), right). Protein chains are shown in space-fill mode with the Env-ELC07 structure coloured as in Fig1; the alternative interface targeting bnAbs in grey.

(D) A model of the ELC07 Fab bound to HIV-1 Env on the viral particle. The Env-ELC07 structure (cartoons, coloured as in Fig1) was docked in the cryo-electron tomography map of HIV-1 spike on in the viral lipid bilayer membrane (EMDB IDs 5019 and 5022<sup>4</sup>, shown as grey surfaces).

**A** T125 PBMCs (1<sup>st</sup> timepoint)



**B** T125 PBMCs (2<sup>nd</sup> timepoint)



**C** Total B cells

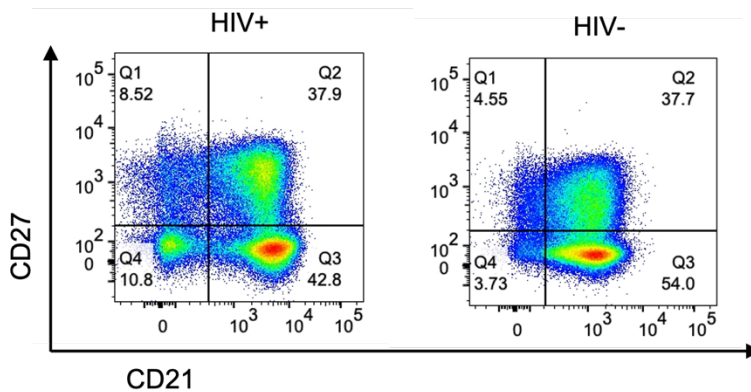


**Figure S3 – B cell subset distributions in the ELC07 bnAb donor – related to Figure 3** (A-B) FACS analysis of total B cells (CD19+ CD4-), IgG+ B cells (CD19+ IgG+ IgM-) and Env+ (CD19+ IgG+ SOSIP+) B cells based on the percentage surface expression of CD27 and CD21 from bnAb donor T125 (A) 1<sup>st</sup> timepoint PBMC and (B) 2<sup>nd</sup> timepoint PBMC (sampled four months apart). (C) FACS analysis of total B cells (CD19+ CD4-) based on the percentage surface expression of CD27 and CD21 from a person living with HIV-1 with viremia and an HIV-1 negative donor.

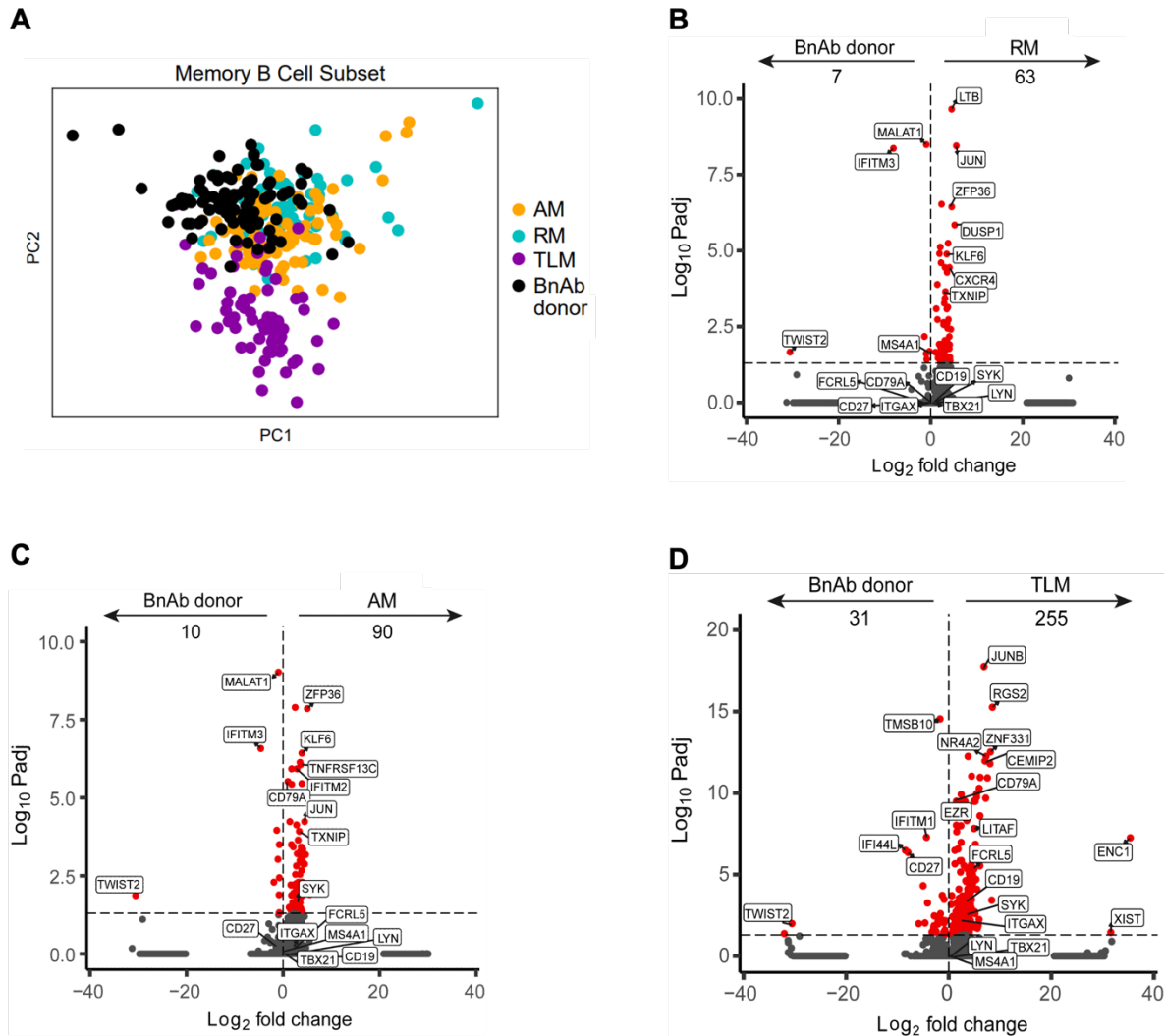


**Figure S4 – Comparison of HIV-1 Env reactive IgG+ B cells from BnAb donor and total memory B cells from the reference donor – related to Figure 4**

(A) PCA visualisation of HIV-1 Env reactive IgG+ B cells from the bnAb donor (black) after integration with resting memory (RM; cyan), activated memory (AM; orange) and tissue-like memory (TLM; purple) IgG+ B cells from a person living with HIV-1 donor with low VL.

(B-D) Volcano plots of DEG between HIV-1 Env reactive IgG+ B cells from the bnAb donor and (B) RM (C) AM and (D) TLM IgG+ B cells. The horizontal dotted line indicates the adjusted p-value threshold for significant DEGs that are highlighted in red and the total number of DEGs is stated underneath each arrow. The top DEGs, as well as genes of interest, are annotated.

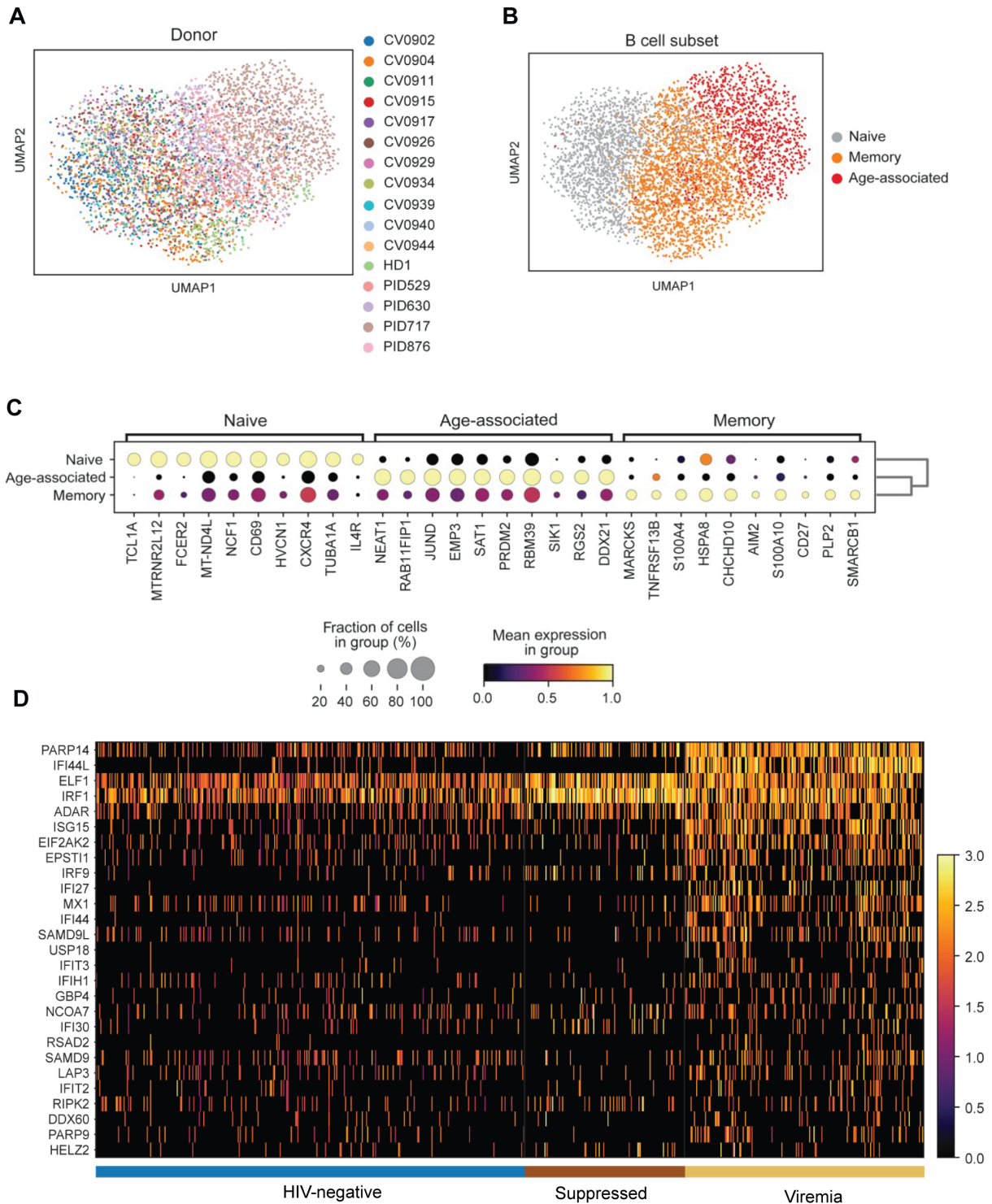


**Figure S5 – Integration of publicly available data from HIV-negative controls and individuals living with HIV-1 viremia– related to Figure 5**

(A-B) UMAP visualisation of B cells integrated from two publicly available scRNA-seq (10x) datasets taken from 11 HIV-negative donors<sup>5</sup> and 2 people living with HIV-1 with viremia, 2 people living with HIV-1 with viral suppression and 1 HIV-negative donor<sup>6</sup>. Coloured by (A) donor ID or (B) Celltypist annotation. (C) Expression of the top 10 DEGs for each B cell subset annotated by Celltypist. The dot size indicates the fraction of cells expressing each particular gene, the dot colour indicates mean gene expression. (D) Expression heatmap of unique leading edge genes from GSEA for hallmark IFN by memory B cells from donors that were HIV-negative (control), suppressed or who had detectable viremia.





**Table S1. Cryo-EM data collection, image processing and model refinement.**

<b>Data collection</b>	
Microscope, operating voltage	Titan Krios G2, 300 keV
Detector	Falcon 4i
Magnification (nominal)	130,000
Pixel size (Å)	0.95
Underfocus range (nominal, μm)	1.3 - 3.1
Number of EER frames per movie	1,674
Total electron fluence (e/Å <sup>2</sup> )	33
Automation software	EPU
Total number of micrograph movies used	31,602
<b>Reconstruction</b>	
Software for 2D classification	cryoSPARC-4.3
Software for 3D classification	Relion-4.1, cryoSPARC-4.3
Software for final reconstruction	cryoSPARC-4.3
Number of initially extracted particles	4,270,949
Number of refined particles	275,291
Symmetry	C1
Global resolution (FSC 0.143, Å)	2.92
Map resolution range (Å)	2.5 - 4.5
Map sharpening B factor	-115.9
<b>Model refinement</b>	
Software for real-space refinement	Phenix 1.21rc1-5084
Model composition	
Number of non-hydrogen atoms	17,517
Number of protein residues	2,113
Number of glycan residues (NAG, BMA, MAN)	67, 4, 4
<i>B</i> factors (Å <sup>2</sup> )	
Protein	54.1
Glycan residues	67.4
Real-space correlation coefficient (CC <sub>mask</sub> , CC <sub>box</sub> , CC <sub>peaks</sub> , CC <sub>volume</sub> )	0.84, 0.73, 0.73, 0.80
R.m.s. deviations	
Bond lengths (Å)	0.004
Bond angles (°)	0.655
Model validation <sup>a</sup>	
MolProbity score	1.59
Clash score	4.95
Poor rotamers (%)	1.46
CaBLAM outliers (%)	2.0
Ramachandran plot quality (%)	
Favored	96.77
Disallowed	0

<sup>a</sup> Assessed using MolProbity (<http://molprobity.biochem.duke.edu/>).

## References

- 1 Min, X. *et al.* Predicting enhancers with deep convolutional neural networks. *BMC Bioinformatics* **18**, 478, doi:10.1186/s12859-017-1878-3 (2017).
- 2 Scharf, L. *et al.* Broadly Neutralizing Antibody 8ANC195 Recognizes Closed and Open States of HIV-1 Env. *Cell* **162**, 1379-1390, doi:10.1016/j.cell.2015.08.035 (2015).
- 3 Pancera, M. *et al.* Structure and immune recognition of trimeric pre-fusion HIV-1 Env. *Nature* **514**, 455-461, doi:10.1038/nature13808 (2014).
- 4 Liu, J., Bartesaghi, A., Borgnia, M. J., Sapiro, G. & Subramaniam, S. Molecular architecture of native HIV-1 gp120 trimers. *Nature* **455**, 109-113, doi:10.1038/nature07159 (2008).
- 5 Stephenson, E. *et al.* Single-cell multi-omics analysis of the immune response in COVID-19. *Nature Medicine* **27**, 904-916, doi:10.1038/s41591-021-01329-2 (2021).
- 6 Wang, S. *et al.* An atlas of immune cell exhaustion in HIV-infected individuals revealed by single-cell transcriptomics. *Emerg Microbes Infect* **9**, 2333-2347, doi:10.1080/22221751.2020.1826361 (2020).